Cell-Surface Bound Nonreceptors and Signaling Morphogen Gradients

By Frederic Y. M. Wan

The patterning of many developing tissues is orchestrated by gradients of signaling morphogens. Included among the molecular events that drive the formation of morphogen gradients are a variety of elaborate regulatory interactions. Such interactions are thought to make gradients robust, i.e., insensitive to change in the face of genetic or environmental perturbations. However just how this is accomplished is a major unanswered question. Recently extensive numerical simulations suggest that robustness of signaling gradients can be achieved through morphogen degradation mediated by cell surface bound nonsignaling receptor molecules (or *nonreceptors* for short) such as heparan sulfate proteoglycans. The present paper provides a mathematical validation of the results from the aforementioned numerical experiments. Extension of a basic extracellular model to include reversible binding with nonreceptors synthesized at a prescribed rate and mediated morphogen degradation shows that the signaling gradient diminishes with increasing concentration of cell-surface nonreceptors. Perturbation and asymptotic solutions obtained for (i) low (receptor and nonreceptor) occupancy, and (ii) high nonreceptor concentration permit more explicit delineation of the effects of nonreceptors on signaling gradients and facilitate the identification of scenarios in which the presence of nonreceptors may or may not be effective in promoting robustness.

1. Introduction

In the early stage of biological development, cells receive positional information, usually from spatially distributed, and (signaling-)receptor bound *morphogens*,

Address for correspondence: Frederic Y.M. Wan, Department of Mathematics, University of California, Irvine, CA 92697-3875, USA; e-mail: fwan@math.uci.edu

DOI: 10.1111/sapm.12030

STUDIES IN APPLIED MATHEMATICS 133:151–181

to adopt different fates resulting in tissue patterning. Morphogens (aka *ligands*) such as Decapentaplegic (*Dpp)* in a Drosophila wing imaginal disc are protein molecules that are synthesized (often at a localized source), transported away from their source and bound to signaling receptors such as Thickveins (*Tkv*) downstream to form a spatial concentration gradient of (signaling) *Dpp-Tkv* complexes. Graded differences in signaling receptor occupancy at different locations underlie the signaling differences that ultimately lead cells down different paths of development.

An important requirement for morphogen gradients is to produce patterns that are not easily altered by genetic or environmental fluctuations. The insensitivity of a system's output to variations in input or system parameters is often termed *robustness*. How this requirement is met has been the subject of a number of recent studies such as [1–12]. Understanding how robustness is attained is important not only for shedding light on the reliability of developing systems, but also for helping to explain the ubiquitous presence of elaborate regulatory schemes in morphogen systems beyond those needed to produce a stable signaling gradient of receptor-morphogen complexes (or simply *bound morphogens*).

The *Drosophila* (*melanogaster*) fruit fly wing imaginal disc for instance is patterned by the morphogen *Decapentaplegic* (*Dpp*), a member of the bone morphogenetic protein (BMP) branch of the transforming growth factor-β (TGF-β) superfamily, and its signaling receptor *Thickveins* (*Tkv*). An in vivo visualization of the bound *Dpp* gradient in a wing imaginal disc is shown in figure 1 of [13]. Figure 2 of the same reference indicates the evolution of the bound morphogen gradient in the wing imaginal disc leading to a tissue pattern that includes an anterior and a posterior wing blade (see also [14]). With *diffusion* as a mechanism for morphogen transport, recent mathematical modeling and analysis of reversible binding and (signaling-)receptor mediated degradation of *Dpp* in the wing imaginal disc in [15–18] showed that the steady state morphogen concentration gradients generated by these models are consistent with available experimental observations [13, 19].

Formation of concentration gradients of different morphogen-receptor complexes is expected to be affected by other known ligand activities including binding with molecular entities (such as heparan sulfate proteoglycans) other than their signaling receptors. Such nonsignaling entities will be called *nonreceptors* since they bind with morphogens but the resulting bound morphogen complexes do not contribute to signaling activities. From this perspective, the presence of nonreceptors reduces the amount of morphogens available for binding with signaling receptors and thereby reduces cell signaling. Effects of nonreceptors have been examined briefly in [5, 20]. In [20], we extended the simple wing disc morphogen model of [17] to include the possibility of morphogen binding with a certain kind of cell-surface bound nonreceptor to investigate their inhibiting effects on the formation and properties of steady state signaling

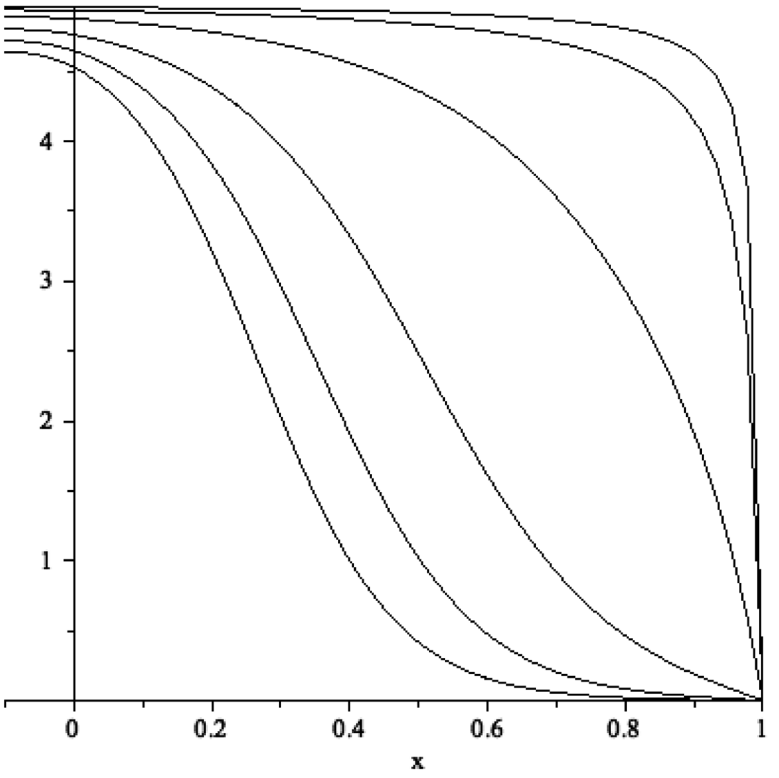

Figure 1. Steady state signaling gradient $\bar{b}(x; Z)$ for $D = 10^{-7}\text{cm}^2/\text{s}$. with $Z = 0$, 1, 2.5, 5, 7.5, and 10 (from top down).

morphogen-receptor gradients and the related transient half life. The new features of that investigation include nonreceptor mediated degradation known to be involved in ligand activities and expected to have substantive effects on ligand gradient formation. In addition to showing the various effect of nonreceptors, the results obtained there have enabled us to clarify a seeming inconsistency of two sets of experimental results in the literature on signaling gradients in Drosophila imaginal disc [21, 22].

Available experimental results (obtained by S. Zhou in A.D. Lander's Lab at UCI) show that *Dpp* synthesis rate in Drosophila imaginal disc doubles when the ambient temperature is increased by 6°C. With such an increase in *Dpp* synthesis rate, the simple models developed in [15–18] would lead to signaling gradients qualitatively different from that at the lower (normal) ambient temperature. Yet, little abnormality in the development of the wing imaginal disc is observed under such a change in ambient temperature (see also [9]). In effect, *Dpp*-mediated patterning of the Drosophila wing appears substantially robust to significant increase in *Dpp* synthesis rate. On the other

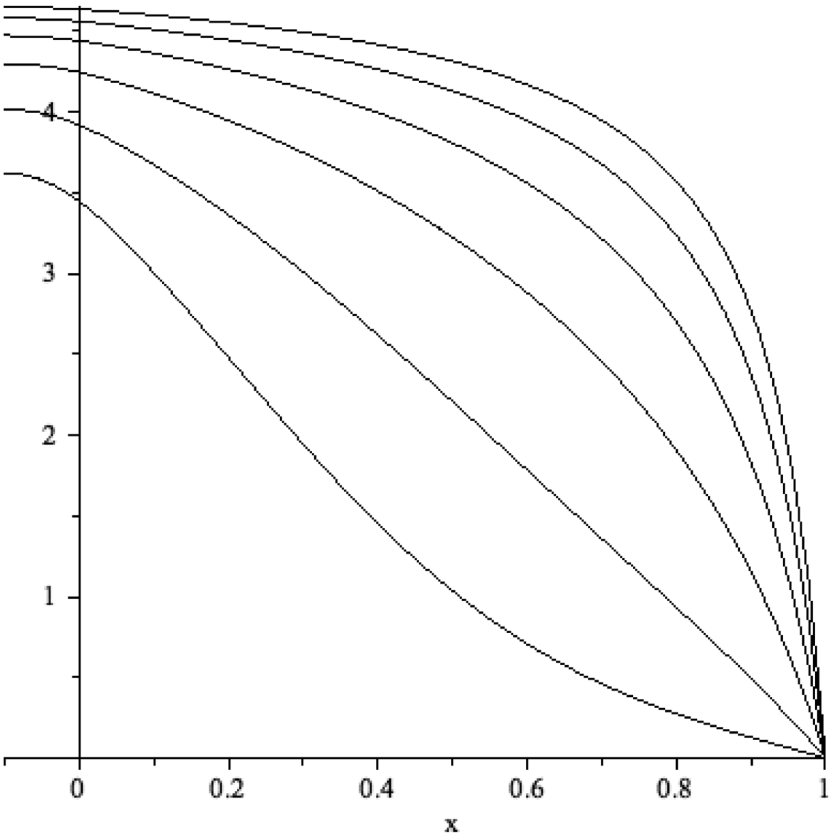

Figure 2. Steady state signaling gradient $\bar{b}(x; Z)$ for $D = 10^{-6}\text{cm}^2/\text{s}$. with $Z = 0$, 1, 2.5, 5, 10, and 20 (from top down).

hand, modification of models such as the one in [17] by the addition of a feedback loop in which receptor synthesis rate is downregulated by an increase in morphogen signaling was found not to lead to robustness (by numerical simulation in [12] and by theoretical analysis in [23]).

Two novel strategies for achieving robustness have been identified by massive simulations in [12]; both involve cell surface nonreceptors mediating a large proportion of overall morphogen degradation. That nonreceptors provide a mechanism for robust signaling gradients with respect to increased *Dpp* synthesis rate is shown in [12] computationally for a portion of the 10^6 biologically realistic sets of parameter values in a six dimensional parameter space. One purpose of the present paper is to provide a theoretical validation of the results of these numerical experiments pertaining to nonreceptors as an agent for robustness complementing the results in [10]. As measured by the *robustness index* introduced in [9, 10, 12], signaling morphogen gradients are

shown to be robust with respect to enhanced morphogen synthesis rates given a sufficiently high concentration of nonreceptors.

For a proof of concept effort, a simplified model of morphogen gradient systems was used in [20] to investigate the effect of nonreceptors. The model assumes prescribed concentrations of receptors and nonreceptors; they are available for binding with *Dpp* if not already occupied. The model in this paper allows both receptors and nonreceptors to be synthesized at a prescribed rate and degrade at a rate proportional to its current concentration as well as to the concentration of bound *Dpp*. As such, it is more realistic than the model in [20]. When there is an abundance of receptors and nonreceptors so that the system is in a state of *low* (*receptor and nonreceptor*) *occupancy*, this paper shows that the two models are to give qualitatively similar results. It is also of considerable interest to see how the present model delimits the applicability of the assumption of fixed concentrations of receptors and nonreceptors.

Given the results of [16], an extracellular model such as the one in this paper is also expected to give results equivalent to those of models that allow for encytosis and exocytosis, such as the one treated in [10]. From a juxtaposition of the analyses in [16] and [17], proofs of well-posedness and other qualitative results for the present extracellular model are expected to be considerably simpler mathematically than that of [10]. The extracellular model also enables us to show more explicitly why nonreceptors may or may not be effective in promoting robustness with respect to an enhanced morphogen synthesis rate. Perturbation and asymptotic solutions appropriate for low receptor and nonreceptor occupancy and for high nonreceptor concentrations display very simply and explicitly how nonreceptors modify the signaling gradients, driving any enhanced signaling gradient toward the distribution prior to enhancement. In addition, the simpler model is expected to make the investigation of various type of feedback mechanisms including that on the nonreceptor synthesis rates more tractable.

As binding with nonreceptors is generic and our method of analysis applies to any gradient in which cell-surface nonreceptor molecules mediate morphogen degradation, our results also offers some insight to why nonreceptors are found almost universally in morphogen gradient systems. Some interesting effects of the freely diffusive nonreceptor molecules have been investigated and reported in [11, 24–26] and references cited therein.

2. A one-dimensional formulation

In this paper, we focus on *Dpp* gradients in the extracellular space of the posterior compartment of a Drosophila wing imaginal disc. (It has been shown in [16] that the inclusion of transcytosis leads only to a re-interpretation of the

system parameters in the final results.) For the purpose of analyzing the effects of nonreceptors, the development of the wing imaginal disc is adequately modeled by a one-dimensional reaction-diffusion problem. In this problem, morphogen is introduced at the rate V_L locally adjacent (and symmetric with respect) to the border, $X = -X_m$, between the *anterior* and *posterior* compartment of the disc, and completely absorbed at the other end, $X = X_{\max}$, the edge of the posterior compartment. The biological development is taken to be uniform in the direction along the compartment border (except possibly for a layer phenomenon at each end) to reflect the fact that the *Dpp* synthesis rate is taken to be uniform in that direction. Extension to a two-dimensional model to allow for nonuniform activities in the apical-basal direction and their implications on robustness have been carried out in [9, 18].

2.1. An extracellular model

Let $[L(X, T)]$ be the concentration of a diffusing morphogen (such as *Dpp*) at time T and distance X toward the wing disc edge normal to the compartment boundary with the localized source spanning $-X_m < X < 0$. As in [17], we take the diffusion of the ligand to be governed by Fick's second law, $\partial[L]/\partial T = D\partial^2[L]/\partial X^2$, D being the diffusion coefficient. We add to this relation the formation and dissociation of ligand-receptor complexes at the binding rate $-k_{on}[L][R]$ and dissociation rate $k_{off}[LR]$. Here $[R]$ is the concentration of signaling *Tkv* receptors for *Dpp*, synthesized at the spatially distributed rate of $V_R(X, T)$, and $[LR]$ is the concentration of ligand-receptor (*Dpp-Tkv*) complexes which degrade at the (receptor-mediated) degradation rate $k_{\text{deg}}[LR]$. In these expressions, k_{on}, k_{deg}, and k_{off} are the binding rate constant, degradation rate constant, and dissociation rate constant, respectively. There is no endocytosis prior to degradation in this formulation. The omission of receptor internalization results in no loss of generality for the purpose of analysis; we have already established in [16] that the boundary value problem (BVP) governing the steady state behavior of a more general systems with receptor internalization can be reduced the same BVP for our simpler system. For the effects of a proteoglycan type nondiffusive (cell-surface bound) nonreceptor concentration $[N(X, T)]$ synthesized at the rate $V_N(X, T)$, we add to these reactions a set of similar activities for the nonreceptor sites resulting in a concentration of ligand–nonreceptor complexes $[LN(X, T)]$ with j_{on}, j_{deg}, and j_{off} being the corresponding rate constants. In this way, we obtain the following nonlinear reaction-diffusion system governing the evolution of the various concentrations $[L]$, $[R]$, $[N]$, $[LR]$, and $[LN]$:

$$\frac{\partial[L]}{\partial T} = D\frac{\partial^2[L]}{\partial X^2} - k_{\text{on}}[L][R] + k_{\text{off}}[LR] - j_{\text{on}}[L][N] + j_{\text{off}}[LN] + V_L, \tag{1}$$

$$\frac{\partial[LR]}{\partial T} = k_{\text{on}}[L][R] - (k_{\text{off}} + k_{\text{deg}})[LR],$$
$$\frac{\partial[R]}{\partial T} = V_R - k_{\text{on}}[L][R] + k_{off}[LR] - k_g[R], \tag{2}$$

$$\frac{\partial[LN]}{\partial T} = j_{\text{on}}[L][N] - (j_{\text{off}} + j_{\text{deg}})[LN],$$
$$\frac{\partial[N]}{\partial T} = V_N - j_{\text{on}}[L][N] + j_{\text{off}}[LN] - j_g[N], \tag{3}$$

where $V_L(X, T)$ is the localized morphogen synthesis rate (centered at and) spanning symmetrically with respect to the border $X = -X_{\min}$ and uniform between the two wing disc compartments. To be specific, we take

$$V_L(X, T) = \bar{V}_L H(-X) = \begin{cases} \bar{V}_L & (-X_m < X < 0) \\ 0 & (0 < X < X_{\max}). \end{cases} \tag{4}$$

With the early stage of the anterior compartment and posterior compartment developing more or less similarly, we consider here only the development in the posterior compartment for which we have the following idealized boundary conditions:

$$X = -X_{\min}: \quad \frac{\partial[L]}{\partial X} = 0, \quad X = X_{\max}: \quad [L] = 0, \tag{5}$$

for all $T > 0$, where the no flux condition at the compartment border being a consequence of symmetry, and the kill end condition at the distal edge, $X = X_{\max}$, of the compartment reflects the assumption of an absorbing edge (which we will occasionally take to be infinitely far away to avoid making such an assumption). For this paper, we consider the case of uniform receptor and nonreceptor synthesis rates, both in space and time with $V_R(X, T) = \bar{V}_R > 0$ and $V_N(X, T) = \bar{V}_N \geq 0$.

Until morphogens being generated at $T = 0$, the biological system was in quiescence so that we have the homogeneous initial conditions

$$T = 0: \quad [L] = [LR] = [LN] = 0, [R] = R_0, [N] = N_0, \tag{6}$$

for $-X_m \leq X \leq X_{\max}$, with

$$R_0 = \frac{\bar{V}_R}{k_g}, \quad N_0 = \frac{\bar{V}_N}{j_g}. \tag{7}$$

from steady state consideration. In the absence of nonreceptor (through $\bar{V}_N = 0$ and therewith $N_0 = 0$), the initial-boundary value problem (IBVP for short) defined by (1)–(6) reduces to the model treated in [17].

2.2. Dimensionless form

To reduce the number of parameters in the problem, we introduce the normalized quantities

$$t = \frac{D}{X_0^2}T, \quad x = \frac{X}{X_0}, \quad Z = \frac{N_0}{R_0}, \quad \ell_M = \frac{X_{\max}}{X_0} \tag{8}$$

$$\{a, b, r\} = \frac{1}{R_0}\{[L], [LR], [R]\}, \quad \{c, n\} = \frac{1}{N_0}\{[LN], [N]\}, \tag{9}$$

$$\{f_0, g_0, h_0, g_r, f_1, g_1, h_1, g_n\} = \frac{X_0^2}{D}\{k_{\text{off}}, k_{\text{deg}}, k_{\text{on}}R_0, k_g, j_{\text{off}}, j_{\text{deg}}, j_{\text{on}}R_0, j_g\}, \tag{10}$$

$$\{\bar{h}_0, \bar{h}_1\} = \frac{X_0^2}{D}\{k_{\text{on}}N_0, j_{\text{on}}N_0, j_g\}, \quad \{\bar{v}_L, \bar{v}_R, \bar{v}_N\} = \frac{X_0^2}{D}\left\{\frac{\bar{V}_L}{R_0}, \frac{\bar{V}_R}{R_0}, \frac{\bar{V}_N}{N_0}\right\}, \tag{11}$$

where X_0 is some typical scale length, taken to be $X_{\max}$ for the finite domain case so that $\ell_M = X_{\max}/X_0 = 1$. With these normalized quantities, we rewrite the IBVP for the five unknowns $[L]$, $[LR]$, $[LN]$, $[R]$, and $[N]$ in the following normalized form

$$\frac{\partial a}{\partial t} = \frac{\partial^2 a}{\partial x^2} - h_0 ar + f_0 b - Zh_1 an + Zf_1 c + \bar{v}_L H(-x), \tag{12}$$

$$\frac{\partial b}{\partial t} = h_0 ar - (f_0 + g_0)b, \quad \frac{\partial r}{\partial t} = \bar{v}_R - h_0 ar + f_0 b - g_r r, \tag{13}$$

$$\frac{\partial c}{\partial t} = h_1 an - (f_1 + g_1)c, \quad \frac{\partial n}{\partial t} = \bar{v}_N - h_1 an + f_1 c - g_n n, \tag{14}$$

with the boundary conditions

$$x = -x_m : \quad \frac{\partial a}{\partial x} = 0, \quad x = \ell_M : \quad a = 0, \tag{15}$$

for all $t > 0$, and the initial conditions

$$t = 0 : a = b = c = 0, \quad r = 1, \quad n = 1, \tag{16}$$

in the interval $-x_m \le x \le \ell_M$.

The IBVP defined by (12)–(16) constitutes a new mathematical model for morphogen activities in the presence of nondiffusive nonreceptors. It will be used to study the effects of such nonreceptor sites on the amplitude and shape of the various steady state ligand concentration gradients and the decay rate of

transient behavior. Our ultimate goal is to see how the presence of a sufficiently high concentration of nonreceptors should make the signaling morphogen gradient $[L\,R]$ robust with respect to an enhanced Dpp synthesis rate.

3. Time-independent steady state

3.1. Reduction

We denote by $\bar{a}(x), \bar{b}(x), \bar{c}(x), \bar{r}(x)$, and $\bar{n}(x)$ the time-independent steady state solution for $a(x,t)$, $b(x,t)$, $c(x,t)$, $r(x,t)$, and $n(x,t)$ of (12)–(16), respectively. For this steady state solution, we have $\partial(\ )/\partial t = 0$ so that the governing partial differential equations and boundary conditions become

$$\bar{a}'' - h_0\bar{a}\bar{r} + f_0\bar{b} - h_1 Z\bar{a}\bar{n} + f_1 Z\bar{c} + \bar{v}_L H(-x) = 0, \tag{17}$$

$$h_0\bar{a}\bar{r} - (f_0 + g_0)\bar{b} = 0, \quad (g_r + h_0\bar{a})\bar{r} - f_0\bar{b} = \bar{v}_R, \tag{18}$$

$$h_1\bar{a}\bar{n} - (f_1 + g_1)\bar{c} = 0, \quad (g_n + h_1\bar{a})\bar{n} - f_1\bar{c} = \bar{v}_N, \tag{19}$$

with

$$\bar{a}'(-x_m) = 0, \quad \bar{a}(\ell_M) = 0, \tag{20}$$

where a prime indicates differentiation with respect to x, i.e., $(\ )' = d(\ )/dx$.

We can solve (18) and (19) for $\bar{b}, \bar{r}, \bar{c}$, and $\bar{n}$ in terms of $\bar{a}$ to get

$$\bar{b}(x) = \frac{\bar{a}(x)}{\alpha_0 + \zeta_0\bar{a}(x)}, \quad \bar{r}(x) = \frac{\alpha_0}{\alpha_0 + \zeta_0\bar{a}(x)}, \tag{21}$$

$$\bar{c}(x) = \frac{\bar{a}(x)}{\alpha_1 + \zeta_1\bar{a}(x)}, \quad \bar{n}(x) = \frac{\bar{\alpha}_1}{\alpha_1 + \zeta_1\bar{a}(x)}, \tag{22}$$

with

$$\alpha_0 = \frac{f_0 + g_0}{h_0}, \quad \alpha_1 = \frac{f_1 + g_1}{h_1} = Z\bar{\alpha}_1, \quad \{\zeta_0, \zeta_1\} = \left\{\frac{k_{\text{deg}}}{k_g}, \frac{j_{\text{deg}}}{j_g}\right\}. \tag{23}$$

The results are then used to obtain from (17) a BVP for $\bar{a}$ alone:

$$\bar{a}'' - \frac{g_0\bar{a}}{\alpha_0 + \zeta_0\bar{a}} - \frac{Zg_1\bar{a}}{\alpha_1 + \zeta_1\bar{a}} + \bar{v}_L H(-x) = 0, \tag{24}$$

$$\bar{a}'(-x_m) = 0, \quad \bar{a}(\ell_M) = 0. \tag{25}$$

For a finite domain, X_0 would normally be $X_{\max}$ so that $\ell_M = 1$.

3.2. Well-posedness

The following theorem ensures the existence of a unique nonnegative monotone decreasing steady state concentration $\bar{a}(x)$:

THEOREM 1. *For positive values of the parameters* $g_0, f_0, h_0, g_1, f_1, h_1, Z, \bar{v}_L, \bar{v}_R$, *and* $\bar{v}_N$, *there exists a nonnegative regular solution* $\bar{a}(x)$ *of the BVP* (24) *and* (25). *The corresponding concentrations* $\{\bar{b}(x), \bar{c}(x), \bar{r}(x), \bar{n}(x)\}$ *can then be calculated from* (21) *and* (22).

Proof: The existence proof is similar to that in [17] for the case without nonreceptors. It suffices to produce an upper solution and a lower solution for the problem in order to apply the known monotone method in [27] (see also [28, 29]). Though upper and lower solutions are similar to those for the case without nonreceptors given in [17], they will be explicitly constructed below to guide us in subsequent derivations of new results on the role of nonreceptors in ensuring the robustness of the signaling ligand gradient $\bar{b}(x)$.

Evidently, $a_\ell(x) \equiv 0$ is a lower solution since

$$-[a_\ell]'' + \frac{g_0 a_\ell}{\alpha_0 + \zeta_0 a_\ell} + \frac{Z g_1 a_\ell}{\alpha_1 + \zeta_1 a_\ell} - \bar{v}_L H(-x)$$
$$= -\bar{v}_L H(-x) \le 0 \quad (-x_m < x < \ell_M), \quad a_\ell'(-x_m) = 0, \quad a_\ell(\ell_M) = 0.$$

For an upper solution, consider

$$a_u(x) = \bar{v}_L \left\{ \ell_M \left(x_m + \frac{\ell_M}{2} \right) - x_m x - \frac{1}{2} x^2 \right\}$$

with $a_u'(-x_m) = 0$ and $a_u(\ell_M) = 0$. From (i) $a_u(-x_m) = \bar{v}_L (\ell_M + x_m)^2 / 2 > 0$, (ii) $a_u'(x) = -\bar{v}_L (x + x_m) < 0$ for $x > -x_m$, and (iii) $a_u(\ell_M) = 0$, we have

$$a_u(x) > 0 \quad (-x_m \le x < \ell_M).$$

It follows that

$$-[a_u]'' + \frac{g_0 a_u}{\alpha_0 + \zeta_0 a_u} + \frac{Z g_1 a_u}{\alpha_1 + \zeta_1 a_u} - \bar{v}_L H(-x)$$
$$= \bar{v}_L + \frac{g_0 a_u}{\alpha_0 + \zeta_0 a_u} + \frac{Z g_1 a_u}{\alpha_1 + \zeta_1 a_u} - \bar{v}_L H(-x)$$
$$> \bar{v}_L - \bar{v}_L H(-x) \ge 0$$

for $-x_m < x < \ell_M$ so that $a_u(x)$ is an upper solution for the BVP for $\bar{a}(x)$. The monotone method assures us that there exists a solution $\bar{a}(x)$ of the BVP (24) and (25) with

$$0 = a_\ell(x) \le \bar{a}(x) \le a_u(x).$$

Since $a_u(x)$ is already known to be positive for $-x_m \le x < \ell_M$, $\bar{a}(x)$ must be nonnegative in the whole solution domain.

To prove uniqueness, let $a_1(x)$ and $a_2(x)$ be two (nonnegative) solutions and $a(x) = a_1(x) - a_2(x)$. Then as a consequence of the ordinary differential equation (ODE) for $a_1(x)$ and $a_2(x)$, the difference $a(x)$ satisfies the following ODE:

$$-a'' + \frac{g_0\zeta_0\alpha_0 a}{(\alpha_0 + \zeta_0 a_1)(\alpha_0 + \zeta_0 a_2)} + \frac{Zg_1\zeta_1\bar{\alpha}_1 a}{(\alpha_1 + \zeta_1 a_1)(\alpha_1 + \zeta_1 a_2)} = 0.$$

Form

$$\int_{-x_m}^{\ell_M} \left[-a'' + \frac{g_0\zeta_0\alpha_0 a}{(\alpha_0 + \zeta_0 a_1)(\alpha_0 + \zeta_0 a_2)} + \frac{Zg_1\zeta_{1\bar{\alpha}1} a}{(\alpha_1 + \zeta_1 a_1)(\alpha_1 + \zeta_1 a_2)} \right] a\,dx = 0.$$

Upon integration by parts, observing continuity of $\bar{a}(x)$ and $\bar{a}'(x)$, and application of the boundary conditions in (25), the relation above may be transformed into

$$\int_{-x_m}^{\ell_M} [a'(x)]^2 dx + \int_{-x_m}^{\ell_M} \left\{ \frac{g_0\zeta_0\alpha_0[a(x)]^2}{(\alpha_0 + \zeta_0 a_1(x))(\alpha_0 + \zeta_0 a_2(x))} + \frac{Zg_1\zeta_1\bar{\alpha}_1[a(x)]^2}{(\alpha_1 + \zeta_1 a_1(x))(\alpha_1 + \zeta_1 a_2(x))} \right\} dx = 0.$$

Both integrands are nonnegative and not identically zero; therefore we must have $a(x) \equiv 0$ and uniqueness is proved. ■

Stability of the steady state solution with respect to small perturbations can be proved by an argument similar to that used in [20] but will be omitted since it is not needed in subsequent developments.

3.3. *Monotonicity and positivity*

We wish to show that free morphogen concentration $\bar{a}(x)$ and the signaling morphogen gradient $\bar{b}(x)$ are positive at all interior points of the interval $(-x_m, \ell_M)$. First we rule out the possibility of any extremum in that interval.

COROLLARY 2. *Under the same hypotheses as those in Theorem 1, the steady state concentration* $\bar{a}(x)$ *does not attain a maximum or minimum in* $(0, \ell_M)$ *and hence is monotone decreasing in that interval.*

Proof: First, it is easy to see that $\bar{a}(x)$ does not have an interior maximum in the interval $0 < x < \ell_M$. If it should have a local maximum at some interior point x_0, then we must have $(\bar{a}'(x_0) = 0$ and) $\bar{a}''(x_0) \leq 0$. However since $\bar{a}(x) \geq 0$ and $v_L(x) = 0$ in $x > 0$, we have

$$\bar{a}'' = \frac{g_0\bar{a}}{\alpha_0 + \varsigma_0\bar{a}} + \frac{Zg_1\bar{a}}{\bar{\alpha}_1 + \zeta_1\bar{a}} \geq 0.$$

It follows that we must have $\bar{a}''(x_0) = 0$ and therewith $\bar{a}(x_0) = 0$. Since x_0 is a maximum point, we must have $\bar{a}(x) = 0$ in $0 < x < \ell_M$. The continuity

requirements imply $\bar{a}(0) = \bar{a}'(0) = 0$. However it is impossible for any nontrivial solution of the ODE (24) to satisfy both of these conditions as well as the boundary condition $\bar{a}'(-x_m) = 0$ unless $\bar{a}(x) \equiv 0$ for all x in $[-x_m, 0]$ as well. However such a free morphogen concentration does not satisfy (24) in the interval $(-x_m, 0)$ where the normalized *Dpp* synthesis rate is a constant $\bar{v}_L$. Hence, $\bar{a}(x)$ does not have a maximum in $(-x_m, \ell_M)$.

Also, $\bar{a}(x)$ does not have a positive interior minimum. If it should have one at x_0 (with $\bar{a}(x_0) > 0$), then it must have an interior maximum at some $x_1 > x_0$ in order for $\bar{a}(x)$ to decrease from $\bar{a}(x_1) > 0$ to $\bar{a}(\ell_M) = 0$. But this contradicts the fact that $\bar{a}(x)$ does not have an interior maximum. There is still the possibility of a local interior minimum $\bar{a}(x_0) = 0$. With $\bar{a}'(x_0) = 0$ at the local minimum, we have $\bar{a}(x) \equiv 0$ which does not satisfy the ODE (24) in the interval $(-x_m, 0)$.

Altogether, the solution $\bar{a}(x)$ of the BVP must be nonnegative and monotone decreasing from $\bar{a}(-x_m) > 0$ to $\bar{a}(\ell_M) = 0$. ■

We can actually prove that the relevant morphogen concentrations are positive for $x < \ell_M$ which we will need in subsequent development.

COROLLARY 3. *Under the hypotheses of Theorem 1, the concentrations* $\bar{a}(x), \bar{b}(x), \bar{c}(x), \bar{r}(x)$, *and* $\bar{n}(x)$ *do not vanish in* $(-x_m, \ell_M)$.

Proof: Suppose $\bar{a}$ vanishes at x_0 in $(-x_m, \ell_M)$ and hence attains a local minimum there (since $\bar{a}(x)$ is nonnegative). However this contradicts Corollary 2 that asserts that $\bar{a}(x)$ does not have an interior minimum. By (21) and (22), the remaining quantities also do not vanish in the same interval. ■

4. Nonreceptor reducing signal gradient concentration

4.1. Low receptor/nonreceptor occupancy

For the signaling gradient to provide positional information that differentiates cell fates, the normalized concentration $b = [LR]/R_0$ should not be nearly uniform (with a steep gradient adjacent to the absorbing edge). It is not difficult to see that signaling gradients would be positionally indifferent if signaling receptors are in such a state of *high receptor occupancy*. For a fixed *Dpp* synthesis rate and a sufficiently high binding rate, we have $\alpha_0 \ll 1$. If α_0 is sufficiently small so that $\alpha_0 + \zeta_0\bar{a}(x) \simeq \zeta_0\bar{a}(x)$ away from the absorbing edge, the expression (21) simplifies to

$$\bar{b} \simeq \frac{1}{\zeta_0} \quad (x < \ell_M) \tag{26}$$

except for a boundary layer adjacent to the absorbing edge where free and bound morphogen concentration rapidly tend decrease to zero. The resulting signaling

bound morphogen complexes given by (26) is positionally undifferentiating. It is clearly unacceptable for the purpose of assigning differential cell fates and tissue patterning.

Positional indifference would not occur if the binding rate is relatively low compared to the receptor and nonreceptor degradation rates so that $\alpha_0 + \zeta_0 \bar{a}(x) \simeq \alpha_0$. In that case, the relation (21) gives $\bar{b} \simeq \bar{a}/\alpha_0$. If in addition, the binding rate of *Dpp* to nonreceptors is also low so that $\alpha_1 + \zeta_1 \bar{a}(x) \simeq \alpha_1$, the ODE (24) can be approximated accurately by

$$[\bar{a}]'' \simeq \mu^2 \bar{a} - \bar{v}_L H(-x), \quad \mu^2 = \mu_0^2 + Z\mu_1^2 \tag{27}$$

with

$$\mu_0^2 = \frac{g_0}{\alpha_0} = \frac{k_{\text{deg}}}{k_{\text{deg}} + k_{\text{off}}} \frac{x_{\max}^2}{D} k_{\text{on}} R_0 \equiv \psi_0, \tag{28}$$

$$Z\mu_1^2 = \frac{g_1}{\alpha_1} Z = \frac{j_{\text{deg}}}{j_{\text{deg}} + j_{\text{off}}} \frac{x_{\max}^2}{D} j_{\text{on}} N_0 \equiv \psi_1. \tag{29}$$

The complementary solutions of the linear ODE (27) are the exponential functions $e^{-\mu x}$ and $e^{\mu x}$. The slope of $\bar{b}(x)$ is then determined by the parameter μ. If $\mu \gg 1$, the signaling gradient for the limiting case of $\ell_M = \infty$ would be too steep and nearly vanishing except for a narrow interval adjacent to the *Dpp* source (see (32)–(34)). Hence, we have the following operational definition of a biologically useful signaling gradient:

DEFINITION 4. *A signaling morphogen gradient $\bar{b}(x)$ is a biologically useful gradient if the dimensionless binding rate constants h_0 and $\bar{h}_1 = Zh_1$ are small so that*

$$\alpha_0 + \zeta_0 \bar{a}(x) \simeq \alpha_0, \quad \alpha_1 + \zeta_1 \bar{a}(x) \simeq \alpha_1, \quad \mu^2 = O(1). \tag{30}$$

A biologically useful signaling gradient is called a biological gradient henceforth.

The first two conditions in (30) ensure the adequacy of (27). For the Drosophila wing imaginal disc, we have $f_0 \ll g_0$ and $f_1 \leq g_1$ so that $g_0/\alpha_0 \simeq h_0$ and $Zg_1/\alpha_1 \simeq \bar{h}_1$. In that case, we have $\mu^2 = \mu_0^2 + Z\mu_1^2 = O(h_0) + O(\bar{h}_1)$. The last condition then ensure that the gradient is sufficiently differentiating and hence biologically useful. A steady state signaling morphogen gradient is in a *state of low receptor occupancy* if the first and second conditions in (30) are satisfied.

4.2. Perturbation solution for small ζ_0 and ζ_1

At low to moderate ligand synthesis rates, a state of low receptor occupancy is quite typical since ζ_0 and ζ_1 are both less than 1 in biological systems of

interest. When binding rates are slow, we expect the first two condition of (30) to hold for moderate values of $\bar{\nu}_L$. For such cases, a perturbation solution of the BVP in ε is appropriate with ε being the larger of ζ_0 and ζ_1. The leading term approximation, $\bar{a}_0(x)$, for $\bar{a}(x)$ is obtained by neglecting the $\bar{a}(x)$ terms in the denominators of (24) and (25) to get

$$[\bar{a}_0]'' = \mu^2 \bar{a}_0 - \bar{\nu}_L H(-x), \quad \bar{a}_0'(-x_m) = 0, \quad \bar{a}_0(\ell_M) = 0, \tag{31}$$

with $\mu^2 = \mu_0^2 + Z\mu_1^2$ as previously defined in (28) and (29). The ODE for $\bar{a}_0$ is identical to (27) and the exact solution of the linear BVP is immediate.

4.2.1. The limiting case of $\ell_M = \infty$. For the limiting case $\ell_M = \infty$, the solution of (31) is

$$\bar{a}_0(x) = \begin{cases} \dfrac{\bar{\nu}_L}{\mu^2}\{1 - e^{-\mu x_m}\cosh(\mu(x + x_m))\} & (-x_m \le x \le 0) \\ \dfrac{\bar{\nu}_L}{\mu^2}\sinh(\mu x_m)e^{-\mu(x+x_m)} & (0 \le x < \infty) \end{cases}, \tag{32}$$

with

$$\bar{b}(x) \sim \frac{\bar{a}_0(x)}{\alpha_0}, \quad \bar{r}(x) \sim 1, \quad \bar{c}(x) \sim \frac{\bar{a}_0(x)}{\bar{\alpha}_1}, \quad \bar{n}(x) \sim 1, \tag{33}$$

$$\alpha_0 \bar{b}(0) \ \sim \bar{\alpha}_1 \bar{c}(0) \sim \bar{a}(0) \sim \ \bar{a}_0(0) = \frac{\bar{\nu}_L}{\mu^2}\sinh(\mu x_m). \tag{34}$$

The explicit leading term perturbation solution (32) for $\bar{a}(x)$ confirms all the properties described in Theorem 1 and Corollaries 2 and 3. In addition, we have by differentiating (32) with respect to Z the following result for the low occupancy case:

PROPOSITION 5. *For a given $\bar{\nu}_L$, the magnitude of the leading term normalized free morphogen concentration $\bar{a}_0(x)$ and the corresponding magnitude of bound morphogen concentrations $\bar{b}_0(x)$ decrease with increasing Z.*

The justification of this proposition may be simplified by observing $\sinh(\mu x_m) \simeq \mu x_m \ll 1$.

4.2.2. The case of a finite ℓ_M. For a finite positive ℓ_M, the exact solution for $\bar{a}_0(x)$ is

$$\bar{a}_0(x) = \begin{cases} \dfrac{\bar{\nu}_L}{\mu^2}\left\{1 - \dfrac{\cosh(\mu\ell_m)}{\cosh(\mu(\ell_M + x_m))}\cosh(\mu(x + x_m))\right\} & (-x_m \le x \le 0) \\ \dfrac{\bar{\nu}_L}{\mu^2}\dfrac{\sinh(\mu x_m)}{\cosh(\mu(\ell_M + x_m))}\sinh(\mu(\ell_M - x)) & (0 \le x \le \ell_M) \end{cases}, \tag{35}$$

with

$$\bar{b}(x) \sim \frac{\bar{a}_0(x)}{\alpha_0}, \quad \alpha_0 \bar{b}(0) \sim \bar{a}(0) \sim \bar{a}_0(0) = \frac{\bar{\nu}_L}{\mu^2} \frac{\sinh(\mu x_m)}{\cosh(\mu(\ell_M + x_m))} \sinh(\mu \ell_M). \tag{36}$$

For $\mu \ell_m \gg 1$, the expression for $\bar{a}_0(x)$ in the signaling range of $0 \le x < \ell_M$ is asymptotically

$$\bar{a}_0(x) \sim \frac{\bar{\nu}_L}{\mu^2} e^{-\mu x} \quad (0 \le x < \ell_M)$$

so that the gradient is effectively a boundary layer adjacent to $x = 0$, steep near $x = 0$ and drop sharply to near zero away from $x = 0$.

We summarize the results of the discussion above in

PROPOSITION 6. *Even if a morphogen system is in a steady state of low receptor occupancy (so that the first two conditions in* (30) *are satisfied), its signaling gradient may not be a biological gradient if the binding rates are not moderate so that the third condition* $\mu^2 = O(1)$ *of* (30) *is not met.*

A morphogen system is said to be in a state of low (receptor and nonreceptor) occupancy if all three conditions in (30) are satisfied.

4.3. The general case

4.3.1. Reduction of signaling morphogen concentration. In this section, we investigate the effects of nonreceptors without the low receptor/nonreceptor occupancy assumption. The following positive result is a local form of what was found in the previous section.

THEOREM 7. *The rate of changes of* $\bar{a}(x, Z)$ *and* $\bar{b}(x, Z)$ *with respect to* Z *are negative:*

$$\frac{\partial \bar{a}}{\partial Z} < 0, \quad \frac{\partial \bar{b}}{\partial Z} < 0.$$

Hence, the presence of nondiffusive nonreceptors generally lowers the amplitude of the morphogen concentration gradients $\bar{a}(x, Z)$ *and* $\bar{b}(x, Z)$ *for all* x *in* $[-x_m, \ell_M)$.

Proof: Let $u(x; Z) = \partial \bar{a}(x; Z)/\partial Z$ in $(-x_m, \ell_M)$ and differentiate all the relations in (24) and (25) with respect to Z to get

$$-\hat{u}'' + \left[\frac{\alpha_0 g_0}{(\alpha_0 + \zeta_0 \bar{a})^2} + \frac{Z \bar{\alpha}_1 g_1}{(\bar{\alpha}_1 + \zeta_1 \bar{a})^2} \right] \hat{u} - \frac{g_1 \bar{a}}{(\bar{\alpha}_1 + \zeta_1 \bar{a})^2} = 0, \tag{37}$$

$$\hat{u}'(-x_{m,Z}) = 0, \quad \hat{u}(\ell_M; Z) = 0. \tag{38}$$

where $\hat{u}(x;Z) = -u(x;Z)$. The existence and uniqueness of the solution of this linear inhomogeneous BVP is assured by the same monotone method used for Theorem 1. The upper solution needed in this case is

$$\hat{u}_u(x) = \frac{g_1 a_m}{\bar{\alpha}_1}\left[\ell_M\left(x_m + \frac{1}{2}\ell_M\right) - x\left(x_m + \frac{1}{2}x\right)\right]$$

with $a_m = \bar{a}(-x_m, Z) > \bar{a}(x, Z)$. The argument that proves Corollary 3 assures us that $\hat{u} > 0$ for all x in $[-x_m, \ell_M)$. Hence, we have $u(x;Z) = \partial\bar{a}(x;Z)/\partial Z = -\hat{u}(x;Z) < 0$ in $[-x_m, \ell_M,)$ so that $\bar{a}(x;Z)$ is a monotone decreasing function of the scaled nonreceptor concentration magnitude Z there.

Unlike the low receptor/nonreceptor occupancy case, $\bar{b}(x;Z)$ is no longer simply proportional to $\bar{a}(x;Z)$ and the behavior of $\bar{b}(x,Z)$ does not follow immediately from the behavior of $\bar{a}(x;Z)$. However, we have readily from the relation (21)

$$\frac{\partial\bar{b}}{\partial Z} = \frac{\alpha_0}{[\alpha_0 + \zeta_0\bar{a}(x)]^2}\frac{\partial\bar{a}}{\partial Z} < 0$$

given that the coefficient of $\partial\bar{a}/\partial Z$ is positive. ■

4.3.2. Increase of convexity. In addition to reducing signaling morphogen concentration, an equally important, if not more important effect of nonreceptors is on the convexity of the signaling gradient. From (24), re-written as

$$\bar{a}'' = \frac{g_0\bar{a}}{\alpha_0 + \zeta_0\bar{a}} + \frac{Zg_1\bar{a}}{\alpha_1 + \zeta_1\bar{a}} - \bar{v}_L H(-x),$$

we see that the presence of the nonreceptors (when $Z > 0$) renders $\bar{a}''(x)$ more positive. The corresponding gradient becomes more convex. Even in an environment of high morphogen synthesis rate and low receptor concentration (resulting in a bound morphogen gradient too uniformly distributed for differential cell fate), a sufficiently high concentration of nonreceptors would make $\bar{a}(x)$ sufficiently convex so that the resulting signaling gradient biological. In the case of a low receptor occupancy, this follows from immediately from $\bar{b}(x) \sim \bar{a}(x)/\alpha_0$. The accurate numerical solutions of the BVP for $\bar{a}(x)$ reported below show that it is also the case for near receptor saturation.

For these numerical solutions, we use in all cases the following set of parameter values:

$$X_{\max} = 0.01\text{cm}, \quad \bar{V}_L = 0.4\mu\text{M/s}, \quad \bar{V}_R = 3\times 10^{-3}\mu\text{M/s}$$
$$k_{\text{on}}R_0 = j_{\text{on}}R_0 = 0.01/\text{s}, \quad j_{\text{off}} = 10\times k_{\text{off}} = 10^{-5}/\text{s}$$
$$k_{\text{deg}} = j_{\text{deg}} = 2\times 10^{-4}/\text{s}, \quad j_g = 10\times k_g = 0.01/\text{s}$$

with $\bar{V}_N = Z\ j_g\bar{V}_R/k_g$ (given $Z = N_0/R_0 = (\bar{V}_N/j_g)/(\bar{V}_R/k_g)$ and Z to be specified in the legends of the figures below). The diffusion coefficient D

that generated the results in Figure 1 was at a relatively slow $10^{-7}\text{cm}^2/\text{s}$. Without nonreceptors, the total steady state receptor concentration is found to be nearly in a state of saturation except in a boundary layer near the absorbing edge $x = 1$. This can be seen from the top graph in Figure 1 giving the normalized bound morphogen concentration $\bar{b}(x)$ in the absence of nonreceptors. Successively lower graphs correspond to the bound morphogen concentration for $Z = 1, 2.5, 5, 7.5,$ and 10. As Z increases from 0, the convexity of the gradient $\bar{b}(x)$ increases, from nearly uniform and flat, to monotone decreasing and concave, to a partially convex gradient. In fact, $\bar{b}(x)$ becomes very much a biological gradient for $Z \geq 5$.

Numerical results for $\bar{b}(x)$ in Figure 2 are for a relatively fast diffusion coefficient of $D = 10^{-6}\text{cm}^2/\text{s}$. With faster diffusion, more morphogen molecules escape binding with receptor and transported to the absorbing edge at $X_{\max}$. Consequently, the graph for $\bar{b}(x)$ in the absence of nonreceptors is more (monotone decreasing and) concave than the corresponding graph in Figure 1. The same faster transport of free morphogen from source also requires more nonreceptors to take away enough morphogen molecules to make $\bar{b}(x)$ biological. The successive lower gradients in Figure 2 correspond to $Z = 0, 1, 2, 5, 5, 10,$ and 20.

In either case, we see that signaling morphogen gradients, nondifferentiating without nonreceptors, become biological gradients in the presence of sufficiently high concentration of nonreceptors. The change is accomplished by the presence of a sufficiently large concentration of nonreceptors binding with most of the free morphogen molecules to drive the signaling morphogen gradient to a state of low receptor occupancy. Such an inference from the limited numerical results will be confirmed mathematically later by an asymptotic solution of the signaling gradient for large Z. It may well be the reason for the presence of a variety of nonreceptors in the wing imaginal disc of Drosophila and other biological entities.

4.4. Fixed receptor and nonreceptor concentrations

The steady state free *Dpp* concentration $\bar{a}(x; Z)$ for the present model is determined by the BVP (24) and (25),

$$\bar{a}'' - \frac{g_0\bar{a}}{\alpha_0 + \zeta_0\bar{a}} - \frac{Zg_1\bar{a}}{\alpha_1 + \zeta_1\bar{a}} + \bar{v}_L H(-x) = 0, \tag{39}$$

$$\bar{a}'(-x_m) = 0, \quad \bar{a}(\ell_M) = 0.$$

The corresponding occupied and unoccupied receptor and nonreceptor concentrations are given by (21)–(23),

$$\bar{b}(x) = \frac{\bar{a}(x)}{\alpha_0 + \zeta_0\bar{a}(x)}, \quad \bar{r}(x) = \frac{\alpha_0}{\alpha_0 + \zeta_0\bar{a}(x)}, \tag{40}$$

$$\bar{c}(x) = \frac{\bar{a}(x)}{\alpha_1 + \zeta_1\bar{a}(x)}, \quad \bar{n}(x) = \frac{\bar{\alpha}_1}{\alpha_1 + \zeta_1\bar{a}(x)}, \tag{41}$$

with

$$\alpha_0 = \frac{f_0 + g_0}{h_0}, \quad \alpha_1 = \frac{f_1 + g_1}{h_1}, \quad \{\zeta_0, \zeta_1\} = \left\{ \frac{k_{\text{deg}}}{k_g}, \frac{j_{\text{deg}}}{j_g} \right\},$$

They are re-stated above to facilitate comparison with the simpler model used in [20].

While R_0 and N_0 were fixed prescribed constants in [20], here they are given in terms of the synthesis rates and degradation rate constants of the receptors and nonreceptors:

$$R_0 = \frac{\bar{V}_R}{k_g}, \quad N_0 = \frac{\bar{V}_N}{j_g}. \tag{42}$$

To facilitate a comparison of the two models, suppose the prescribed R_0 and N_0 in [20] are as given by (42). In that case, the only differences between the two models consist of the appearance of the two factors $\zeta_0 = k_{\text{deg}}/k_g$ and $\zeta_1 = j_{\text{deg}}/j_g$, the bound and free degradation rate ratios for receptors and nonreceptors, respectively, in the ODE (39) for $\bar{a}(x)$ and the four auxiliary relations (40) and (41). For the simpler and less realistic model of [20], these ratios were absent from the corresponding relations, i.e., they were replaced in all these relations by 1 instead.

Since we have typically $\zeta_0 \ll 1$ and $\zeta_1 \ll 1$, the principal consequence of working with the less realistic model of [20] is a resulting concentration gradient less convex than the more realistic model. Aside from this obvious difference, the replacement of fixed receptor and nonreceptor concentrations by prescribed synthesis rates and degradation rates of these binding sites moves the biological development more toward a state of low receptor occupancy to result in a more useful signaling gradient. Even if $\bar{a}(x)$ is not small compared to α_0 and/or α_1, the presence of the factors ζ_0, and ζ_1 helps to make the terms involving $\bar{a}(x)$ in the denominators of the various fractions to be smaller and more likely to be negligible, with the corresponding morphogen gradients more likely to be in a state of low receptor occupancy.

5. High nonreceptor concentration

5.1. Asymptotic solution in $\varepsilon^2 = 1/Z$

The level of nonreceptors needed to maintain a signaling morphogen gradient that is biologically realistic varies depending on the particular morphogen system as illustrated in the numerical examples in the last section. When morphogen synthesis rate is high and the signaling receptor synthesis is low, a large nonreceptor-to-receptor ratio (so that $Z = N_0/R_0 \gg 1$) is needed to accomplish this task. For a high nonreceptor concentration, a perturbation

solution of the BVP for $\bar{a}(x)$ defined by (24)–(25) in the parameter $\varepsilon^2 = 1/Z$ offers considerable insight to the role of nonreceptors in morphogen gradient systems.

Upon dividing through by Z, the BVP for $\bar{a}$ becomes

$$\varepsilon^2 \bar{a}'' = \varepsilon^2 \frac{g_0 \bar{a}}{\alpha_0 + \zeta_0 \bar{a}} + \frac{g_1 \bar{a}}{\alpha_1 + \zeta_1 \bar{a}} - \varepsilon^2 \bar{v}_L H(-x), \quad \bar{a}'(-x_m) = 0, \quad \bar{a}(\ell_M) = 0. \tag{43}$$

An exact solution of this problem is possible. The method of matched asymptotic expansions is appropriate for the singular perturbation structure of (43). However, neither would not be particularly informative. To the extent that we expect a sufficiently high nonreceptor concentrations should drive gradient system to a state of low receptor occupancy, we work here with the following regular perturbation solution:

$$\bar{a}(x;\varepsilon) = \sum_{n=0}^{\infty} A_n(\xi)\varepsilon^n, \quad \xi = \sqrt{Z}x = \frac{x}{\varepsilon}.$$

with

$$\bar{a}'(x,\varepsilon) = \frac{1}{\varepsilon}\frac{d\bar{a}}{d\xi} \equiv \frac{1}{\varepsilon}\bar{a}^{\cdot}$$

The leading term of the expansion is determined by

$$A_0^{\cdot\cdot} = \frac{g_1 A_0}{\alpha_1 + \zeta_1 A_0} - \bar{v}_\varepsilon H(-\xi), \quad A_0^{\cdot}\left(-\frac{x_m}{\varepsilon}\right) = 0, \quad A_0\left(\frac{\ell_M}{\varepsilon}\right) = 0, \tag{44}$$

with $\bar{v}_\varepsilon = \varepsilon^2 \bar{v}_L$. For the method of match asymptotic expansions, we have $\ell_M/\varepsilon = \ell_M\sqrt{Z} = \sqrt{Z} \to \infty$ when we take the limit $\varepsilon \to 0$ (so that x tending to the the absorbing edge (at $x \to 1$) corresponds to $\xi \to \infty$). On the other hand, the span of the local morphogen source is much shorter than the span of the posterior compartment (in the distal direction) so that $x_m \ll 1$. It is more convenient to keep $x_m/\varepsilon = x_m\sqrt{Z} \equiv \xi_m$ finite in the development below.

5.2. Low nonreceptor occupancy

For low (nonreceptor) occupancy, we have $A_0 \sim a_0$ with

$$a_0^{\cdot\cdot} = \mu_1^2 a_0 - \bar{v}_\varepsilon H(-\xi), \quad a_0^{\cdot}\left(-\frac{x_m}{\varepsilon}\right) = 0, \quad a_0\left(\frac{\ell_M}{\varepsilon}\right) = 0, \tag{45}$$

where $(\,)^{\cdot} = d(\,)/d\xi$. For the limiting case of $\ell_M/\varepsilon = \infty$, the exact solution of linear BVP (45) is

$$\bar{a}(x) \sim A_0(\xi) = \begin{cases} \dfrac{\bar{\nu}_L}{Z\mu_1^2}\{1 - e^{-\mu_1\sqrt{Z}x_m}\cosh(\mu_1\sqrt{Z}(x + x_m))\} \\ \quad \sim \dfrac{\bar{\nu}_L}{2Z\mu_1^2}\{2 - e^{\mu_1\sqrt{Z}x}\} \quad (-\xi_m \le \xi \le 0) \\ \dfrac{\bar{\nu}_L}{Z\mu_1^2}\sinh(\mu_1\sqrt{Z}x_m)e^{-\mu_1\sqrt{Z}(x+x_m)} \\ \quad \sim \dfrac{\bar{\nu}_L}{2Z\mu_1^2}e^{-\mu_1\sqrt{Z}x} \quad (0 \le \xi < \infty) \end{cases} . \tag{46}$$

5.3. Low receptor occupancy

The approximate solution (46) for $\bar{a}(x)$ was obtained with only two restrictions: $Z = N_0/R_0 \gg 1$ and $\alpha_1 \gg \zeta_1\bar{a}(x) \simeq \zeta_1 A_0(x)$. The signaling *Dpp* gradient,

$$\bar{b}(x) = \frac{\bar{a}(x)}{\alpha_0 + \zeta_0\bar{a}(x)},$$

may be in a state of either low or high occupancy. For the case of *low receptor occupancy*, we have

$$\bar{b}(x) \simeq \frac{\bar{a}(x)}{\alpha_0} \sim \frac{\bar{\nu}_L}{\alpha_0 Z\mu_1^2}\sinh(\mu_1\sqrt{Z}x_m)e^{-\mu_1\sqrt{Z}(x+x_m)}$$
$$\sim \frac{\bar{\nu}_L}{2\alpha_0 Z\mu_1^2}e^{-\mu_1\sqrt{Z}x} \quad (0 \le \xi < \infty). \tag{47}$$

For a fixed normalized morphogen synthesis rate $\bar{\nu}_L$, it is seen from the expression (47) that more nonreceptors, i.e., increasing Z, would

(i) reduce the magnitude of the signaling gradient,
(ii) make the slope of the gradient more negative, and
(iii) make the curvature of the gradient more convex.

Since $\bar{b}(x)$ is approximately proportional to the morphogen synthesis rate, increasing $\bar{\nu}_L$ simply increase the gradient magnitude proportionately.

5.4. High receptor occupancy

For *high receptor occupancy*, the expression for $\bar{b}(x)$ does not simplifies. We have instead of (47) the more complicated expression

$$\bar{b}(x) \sim \frac{\bar{\nu}_L}{2Z\mu_1^2}\frac{e^{-\mu_1\sqrt{Z}x}}{\alpha_0 + \zeta_0\bar{\nu}_L e^{-\mu_1\sqrt{Z}x}/2Z\mu_1^2} \quad (0 \le \xi < \infty). \tag{48}$$

For a fixed Z and $\bar{v}_L$ sufficiently large, the quantity $\zeta_0 \bar{v}_L e^{-\mu_1\sqrt{Z}x}/2Z\mu_1^2$ would not be small compared to α_0 at least for x near 0.

On the other hand, for a fixed $\bar{v}_L$, the term $\zeta_0 \bar{v}_L e^{-\mu_1\sqrt{Z}x}/2Z\mu_1^2$ decreases with increasing Z. For a sufficiently large Z, this term would become negligibly small compared to α_0 so that the gradient system would be in a state of low receptor occupancy. As such, nonreceptors play two important roles in morphogen systems:

PROPOSITION 8. *In addition to reducing the strength of the signaling gradient and steepening its downward slope, the presence of a sufficiently large concentration of nonreceptors helps to render the gradient more convex by driving the system toward a state of low receptor occupancy.*

6. Nonreceptors and robustness

6.1. Sensitivity of signaling gradient to enhanced morphogen synthesis

Normal development of wing imaginal disc and other biological organism may be altered by an enhanced morphogen synthesis rate stimulated by environmental or other epigenetic changes. For example, *Dpp* synthesis rate in Drosophila imaginal disc doubles when the ambient temperature is increased by 6 °C (see Section 1). Typically, an enhanced morphogen synthesis rate alters the magnitude and shape of the signal gradient and hence the cell fate at each spatial location. For gradient systems in a state of low (receptor) occupancy, we see from the explicit solution (32) and (34) of the BVP for $\bar{a}(x)$ that the signaling gradient $\bar{b}(x)$ is proportional to $\bar{v}_L$ For the more general case without the restriction of low (receptor) occupancy, we prove presently that $\bar{a}(x)$ and $\bar{b}(x)$ are increasing functions of $\bar{v}_L$.

Let $v(x;\bar{v}_L) = \partial\bar{a}/\partial\bar{v}_L$ and differentiate all the relations in (24) and (25) with respect to $\bar{v}_L$ to get

$$-v'' + \left[\frac{\alpha_0 g_0}{(\alpha_0 + \zeta_0\bar{a})^2} + \frac{Z\bar{\alpha}_1 g_1}{(\bar{\alpha}_1 + \zeta_1\bar{a})^2}\right] v - H(-x) = 0, \tag{49}$$

$$v'(-x_m;\bar{v}_L) = 0, \quad v(\ell_M;\bar{v}_L) = 0. \tag{50}$$

The proof of the existence of a unique solution for this linear BVP is again straightforward; the upper solution needed in this case is

$$v_u(x) = \left[\ell_M\left(x_m + \frac{1}{2}\ell_M\right) - x\left(x_m + \frac{1}{2}x\right)\right].$$

The unique solution for $v(x;\bar{v}_L)$ enables us to prove the following proposition:

PROPOSITION 9. *Under the same hypotheses as Theorem 1,* $\bar{a}(x;\bar{v}_L)$ *and* $\bar{b}(x;\bar{v}_L)$ *are monotonically increasing functions of the normalized morphogen synthesis rate parameter* $\bar{v}_L = v_L$.

Proof: The same argument that proves Corollary 3 also allows us to prove $v > 0$ for all x in $(-x_m, \ell_M)$ so that $\partial\bar{a}(x;\bar{v}_L)/\partial\bar{v}_L > 0$ in $[-x_m, \ell_M,)$; hence, $\bar{a}(x;\bar{v}_L)$ is an increasing function of $\bar{v}_L$. From the relation (21), we have

$$\frac{\partial\bar{b}}{\partial\bar{v}_L} = \frac{\alpha_0}{[\alpha_0 + \zeta_0\bar{a}(x)]^2}\frac{\partial\bar{a}}{\partial\bar{v}_L}. \tag{51}$$

It follows that $\bar{b}$ is an increasing function of $\bar{v}_L$ since both $\partial\bar{a}/\partial\bar{v}_L$ and its coefficient in (51) are positive. ■

6.2. *Diminishing enhancement of* [*L R*] *with more nonreceptors*

Evidently, an abnormal enhancement of morphogen synthesis rate is undesirable for normal development as it always enhances the signaling gradient whether it remains differentiating. We know from the explicit solution (32) and (34) of the BVP for $\bar{a}(x)$ that for a fixed $\bar{v}_L$, however large, the signaling gradient $\bar{b}(x)$ is a decreasing function of Z. For the more general case without the restriction of low (receptor) occupancy, we have already proved in Theorem 7 that $\bar{a}(x)$ and $\bar{b}(x)$ are both monotone decreasing functions of Z. Thus, nonreceptors has a role in reducing the sensitivity of signaling gradients to enhanced morphogen synthesis and thereby offers a possible mechanism for robustness of the signaling gradient, confirming what is suggested by the numerical experiments of [12].

However, Theorem 7 on its own, while a step in the right direction, does not assure robustness. For one thing, it is not quantitative in the reduction of the enhanced signaling gradient $\tilde{b}(x)$. Nor does a sufficient increase in Z necessarily brings $\tilde{b}(x)$ back down to $\bar{b}(x)$. More specifically, let $\bar{b}(x, Z)$ and $\tilde{b}(x, Z)$ be the normalized signaling morphogen-receptor gradients for morphogen synthesis rate $\bar{V}_L$ and $\tilde{V}_L = 2\bar{V}_L$, respectively, for a given level of nonreceptor-to-receptor ratio Z. We know (at least for the low occupancy case) the difference $\tilde{b}(x, 0) - \bar{b}(x, 0)$ would be significant. But what about $\tilde{b}(x, Z) - \bar{b}(x, 0)$ for a prescribed Z? Would it be uniformly small to a prescribed tolerance? From the explicit solution for the low receptor occupancy case, we see that the addition of nonreceptors not only changes the magnitude of the signaling gradient, but also its slope and convexity. The different would not be uniform in x or proportional to $\bar{v}_L$. Hence, there would not be a value Z for which $\tilde{b}(x, Z) = \bar{b}(x, 0)$. Even in a range of x where the difference in signal $\tilde{b}(x, Z) - \bar{b}(x, 0)$ remains small, the difference, $\tilde{x} - \bar{x}$, of locations where $\tilde{b}(\tilde{x}, Z) = \bar{b}(\bar{x}, 0) = b$ would not be small when the slope of the two gradients change slowly. In that case the pattern developed would still be

significantly different since the cell type that was at $\bar{x}$ is now at some distance away at $\tilde{x}$. These observations suffice to suggest that we need one or more quantitative and global measures of robustness that safeguard against such unwanted developments.

6.3. Robustness index

6.3.1. Root-mean-square signaling differential. A rather natural global measure of signaling gradient robust is the following *signal robustness index* R_b corresponding to the root mean square of the deviation between the normalized bound morphogen concentration $[LR]/R_0$ for $\bar{V}_L$ without nonreceptors, denoted previously by $\bar{b}(x, 0)$, and the same quantity for $\tilde{V}_L = 2\bar{V}_L$ with a nonzero nonreceptor-to-receptor ratio Z, denoted previously by $\tilde{b}(x, Z)$:

$$R_b(Z) = \frac{1}{b_h - b_\ell}\sqrt{\frac{1}{x_\ell - x_h}\int_{x_h}^{x_\ell}[\tilde{b}(x, Z) - \bar{b}(x, 0)]^2 dx}, \tag{52}$$

where $0 \le b_\ell \equiv \bar{b}(x_\ell, 0) < \bar{b}(x_h, 0) \equiv b_h \le \bar{b}_0(0)$, with $0 \le x_h < x_\ell \le \ell_M = 1$. The quantities x_ℓ and x_h (or b_ℓ and b_h) may be chosen away from the extremities to minimize the effects of outliers.

For the morphogen system in a state of low receptor occupancy, we have from the following leading term asymptotic solution for $\bar{b}(x, 0)$ and $\tilde{b}(x, Z)$:

$$\bar{b}(x, 0) \sim \frac{\bar{v}_L}{\alpha_0\mu_0^2}\frac{\sinh(\mu_0 x_m)\sinh(\mu_0(\ell_M - x))}{\cosh(\mu_0(\ell_M + x_m))}, \quad (0 \le x \le \ell_M) \tag{53}$$

$$\tilde{b}(x, Z) \sim \frac{2\bar{v}_L}{\alpha_0\mu^2}\frac{\sinh(\mu x_m)\sinh(\mu(\ell_M - x))}{\cosh(\mu(\ell_M + x_m))}. \quad (0 \le x \le \ell_M) \tag{54}$$

An explicit expression can be obtained for R_b when the leading term perturbation solutions are applicable. In particular, we have for $x_\ell = 1$ and $x_h = 0$

$$\begin{aligned} R_b(0) &= \frac{1}{\bar{b}(0, 0)}\sqrt{\int_0^1 [\tilde{b}(x, 0) - \bar{b}(x, 0)]^2 dx} \\ &\sim \frac{1}{\sinh(\mu_0)}\sqrt{\int_0^1 [\sinh(\mu_0(1 - x))]^2 dx} \\ &= \frac{1}{\sinh(\mu_0)}\sqrt{\frac{1}{2}\left(\frac{\sinh(2\mu_0)}{2\mu_0} - 1\right)}. \end{aligned} \tag{55}$$

For a gradient system with the parameter values given in Table 1 except with $\bar{V}_L = 0.005\mu$M/s.(instead of $\bar{V}_L = 0.05\mu$M/s), the steady state is in low receptor occupancy. For this case, the approximate solution for $R_b(0)$ given by (55) is $0.3943\cdots$ while accurate numerical solutions of the BVP for $\bar{a}(x)$ gives

Table 1

$\bar{V}_L = 0.05\mu\text{M/s}, \quad \bar{V}_R = 4 \times 10^{-2}\mu\text{M/s}, \quad k_{\text{deg}} = j_{\text{deg}} = 2 \times 10^{-4}/\text{s},$
$k_{\text{off}} = 10^{-6}/\text{s} = j_{\text{off}} \times 10^{-1}, \quad k_g = 10^{-3}/\text{s} = j_g \times 10^{-1}, \quad X_{\max} = 0.01\text{cm}.$
$k_{\text{on}} R_0 = j_{\text{on}} R_0 = 0.01/\text{s}, \quad D = 10^{-7}\text{cm}^2/\text{s}, \quad X_m = 0.001\text{cm}$

$Z = N_0/R_0$	$\tilde{a}_0(Z)$	$\tilde{b}_0(Z)$	$\tilde{r}_0(Z)$	$\tilde{n}_0(Z)$	$R_b(Z)$	$R_x(Z)$
0	0.0780	2.1848	0.5630	0.9309	0.4269	0.2590
0.25	0.0625	1.9169	0.6166	0.9438	0.2513	0.1507
0.5	0.0531	1.7274	0.6545	0.9519	0.1437	0.0783
1	0.0417	1.4651	0.7070	0.9618	0.0665	0.0656
2	0.0301	1.1516	0.7697	0.9722	0.1698	0.1733

Table 2

$\bar{V}_L = 0.4\mu\text{M/s}, \quad \bar{V}_R = 4 \times 10^{-2}\mu\text{M/s}, \quad k_{\text{deg}} = j_{\text{deg}} = 2 \times 10^{-4}/\text{s},$
$k_{\text{off}} = 10^{-6}/\text{s} = j_{\text{off}} \times 10^{-1}, \quad k_g = 10^{-3}/\text{s} = j_g \times 10^{-1}, \quad X_{\max} = 0.01\text{cm}.$
$k_{\text{on}} R_0 = j_{\text{on}} R_0 = 0.01/\text{s}, \quad D = 10^{-7}\text{cm}^2/\text{s}, \quad X_m = 0.001\text{cm}$

$Z = N_0/R_0$	$\tilde{a}_0(Z)$	$\tilde{b}_0(Z)$	$\tilde{r}_0(Z)$	$\tilde{n}_0(Z)$	$R_b(Z)$	$R_x(Z)$
0	1.4666	4.6793	0.0641	0.4172	0.2412	0.2426
0.25	0.9796	4.5348	0.0931	0.5173	0.1094	0.1191
0.5	0.7298	4.3948	0.1210	0.5900	0.0342	0.0335
0.75	0.5872	4.2693	0.1461	0.6413	0.1262	0.1180
1	0.4954	4.1567	0.1687	0.6794	0.2047	0.1961

0.4052 for a percentage error of less than 3%. The comparison serves to validate the numerical simulation code that generated the results in Tables 1 and 2.

Our main interest however is in the numerical values of R_b for specific sets of system parameter values to illustrate possible robustness of the signaling gradients in the presence of nonreceptors. This type of numerical results are given for the two examples in Tables 1 and 2. For these examples, the relevant morphogen systems are not in a state of low receptor occupancy. The use of the approximate signaling robustness index based on the leading term perturbation solution (53)–(54) would not be appropriate and hence not discussed further. On the other hand, numerical solutions for $\bar{a}(x; Z)$ and $\tilde{a}(x; Z)$ the corresponding numerical evaluation of $R_b(Z)$ are straightforward. (See with the numerical results discussed in the next section.)

6.3.2. Root-mean-square displacement differential. The signal robustness index R_b is not the only measure of the deviation from normal development due to morphogen synthesis rate enhancement (doubling in our examples). Given

an existing genetic program for individual cells, a more relevant measure of robustness may be the displacement of the same level of morphogen-receptor complex concentration due to a change of morphogen synthesis rate. Let $\bar{b}(x, Z)$ and $\tilde{b}(x, Z)$ again be the normalized signaling morphogen-receptor gradients at location x for morphogen synthesis rate $\bar{V}_L$ and $\tilde{V}_L = 2\bar{V}_L$, respectively. Let $\bar{x}$ and $\tilde{x}$ be the corresponding location where they attain the value b, i.e., $\bar{b}(\bar{x}, 0) = \tilde{b}(\tilde{x}, Z) = b$. With a change of ligand synthesis rate, $\tilde{x}$ is generally different from $\bar{x}$ with $\tilde{x} - \bar{x} = \Delta x$. The root-mean-square of Δx over the range of b would be another meaningful measure of robustness:

$$R_x(Z) = \frac{1}{x_\ell - x_u}\sqrt{\frac{1}{b_u - b_\ell}\int_{b_\ell}^{b_u}(\tilde{x} - \bar{x})^2 db}. \tag{56}$$

As mentioned previously, a substantial Δx corresponds to a significant displacement of the cell fate normally at location $\bar{x}$ to a new location $\tilde{x}$. To minimize the effects of outliers, we may limit the range of b to be the interval (b_ℓ, b_u) with $0 \le b_\ell < b_u \le \bar{b}(0; 0)$, e.g., $b_\ell = \bar{b}(0; 0)/10$ and $b_u = 9\bar{b}(0; 0)/10$.

Evidently, R_x should be as small as possible to minimize the deviation from the normal gradient with $R_x(Z) = 0$ being no change. Since $\tilde{b}(x, Z)$ is a monotone decreasing function of Z, we expect $R_x(Z)$ to first decrease as Z increases from 0 reaching a minimum at some optimal Z_{op}. From that point on, $R_x(Z)$ is expected to increase with Z. An important question would be whether there is a range of Z values for which $R_x(Z)$ is in the acceptable range of $R_x(Z) < 0.2$. Some numerical results for $R_x(Z)$ for several choice values of Z are reported in Tables 1 and 2 (see next section for a discussion of these results) for the same two examples considered previously for $R_b(Z)$.

It should be noted that unlike the numerical evaluation of $R_b(Z)$, the numerical evaluation of $R_x(Z)$ is more complicated and will be addressed in the next section. If the morphogen system is in a state of low occupancy, we can again use the perturbation solution (35) and (36) for a simpler evaluation of $R_x(Z)$. In particular, we have for $x_\ell = 1$ and $x_u = 0$

$$R_x(Z) = \sqrt{\frac{1}{\bar{b}_0}\int_0^{\bar{b}_0}(\tilde{x} - \bar{x})^2 db},$$

where $\bar{b}_0 = \bar{b}(0, 0)$. For $\mu \gg 1$, we have

$$\bar{b}(x) \sim B_0(Z)e^{-\mu x}, \quad B_0(Z) = \frac{\bar{\nu}_L}{2\alpha_0\mu^2}\left(1 - e^{-2\mu x_m}\right)$$

with $\mu^2 = \mu_0^2 + Z\mu_1^2$. It follows that

$$R_x(Z) \sim \frac{\ln(2)}{\mu}, \quad R_x(0) \sim \frac{\ln(2)}{\mu_0}.$$

6.4. Numerical results for robustness indices

6.4.1. Numerical evaluation of $R_x(Z)$. While the numerical evaluation of $R_b(Z)$ is straightforward, the corresponding evaluation of $R_x(Z)$ requires some finesse. To the extent that the governing BVP has been formulated in terms of $\bar{a}(x;Z)$, we first re-write $R_x(Z)$ (as defined in (56)) as

$$R_x(Z) = \frac{1}{x_\ell - x_u}\sqrt{\frac{\alpha_0}{b_u - b_\ell}\int_{a_\ell}^{a_u}\left(\frac{\tilde{x}-\bar{x}}{\alpha_0+\zeta_0 a}\right)^2 da}. \tag{57}$$

It remains to develop a numerical method for determining $\tilde{x}(a;Z)$ and $\bar{x}(a;Z)$ for the signaling gradient range $0 \le a \le \bar{a}(0;0) \equiv \bar{a}_0$ (corresponding to $0 \le x \le 1$). While it is possible to formulate a self-contained algorithm for this purpose, it is numerically less challenging to use an approach that takes advantage of three pieces of information we already obtained while computing $R_b(Z)$, namely, $\bar{v}_1 = \bar{a}'(1;0)$, $\tilde{v}_1 = \tilde{a}'(1;0)$ and $\tilde{v}_z = \tilde{a}'(1;Z)$ (for a prescribed $Z > 0$) where $\tilde{a}(x;Z)$ is the solution of the BVP with $\tilde{V}_L$ instead of $\bar{V}_L$.

Let $w(x;Z) = (da/dx)^{-1}$ so that

$$\frac{dx}{da} = w(x;Z). \tag{58}$$

With

$$\frac{dw}{da} = \frac{dw/dx}{da/dx} = w\frac{d}{dx}\left(\frac{1}{da/dx}\right) = -w^3\frac{d^2a}{dx^2}$$

(where we have used a instead of $\bar{a}$ to allow for the possibility of different morphogen synthesis rate), we get from (39) a second equation for w and x as functions of a for $0 < a < \bar{a}_0$:

$$\frac{dw}{da} = -w^3\left(\frac{g_0 a}{\alpha_0+\zeta_0 a} + Z\frac{g_1 a}{\alpha_1+\zeta_1 a}\right) \tag{59}$$

given that there is no morphogen synthesis in the range $0 < x < 1$. The two first-order ODE (58) and (59) are augmented by two initial conditions:

$$x(0;Z) = 1, \quad w(0;Z) = w_1. \tag{60}$$

corresponding to $a(x=1;Z) = 0$ and $a'(x=1;Z) = 1/w(a=0;Z)$. For the information needed to calculate $R_x(Z)$, we have to solve the IVP defined by (58)–(60) for three different values of w_1, $1/\bar{v}_1$, $1/\tilde{v}_1$, and $1/\tilde{v}_z$, to get $\bar{x}(a;0)$, $\tilde{x}(a;0)$, and $\tilde{x}(a;Z)$.

6.4.2. Two numerical examples. For the particular set of parameter values given in Table 1, we have $\{\alpha_0 = 0.0201, \bar{\alpha}_1 = 0.021\}$and $\{\zeta_0 = 0.2, \zeta_1 = 0.02\}$. Together with the results on $\tilde{r}_0(Z) = \tilde{r}(0;Z)$ and $\tilde{n}_0(Z) = \tilde{n}(0;Z)$ reported in the table, we see that the steady state solution for the enhanced synthesis rate is only with low nonreceptor occupancy but *not* low receptor occupancy (or

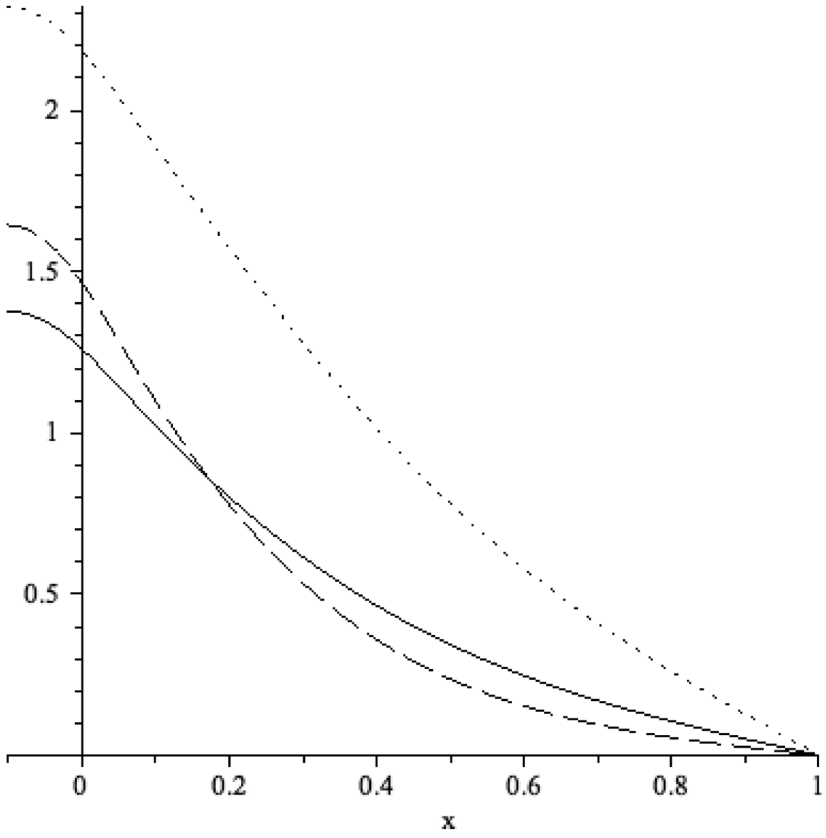

Figure 3. Signaling gradients for system reported in Table 1 for $Z = 1$. (solid $= \bar{b}(x, 0)$, dashed $= \tilde{b}(x, 1)$, dots $= \tilde{b}(x, 0)$).

near receptor saturation). The use of the leading term perturbation solution (53)–(54) is therefore not appropriate. Nevertheless, the signaling gradient $\bar{b}_0(0) = \bar{b}(0; 0)$ and $\tilde{b}_0(Z) = \tilde{b}(0; Z)$ are suitably convex to be biologically realistic but with the enhanced signaling gradient $\tilde{b}_0(0) = \tilde{b}(0; 0)$ significantly different from the normal gradient $\bar{b}_0(0) = \bar{b}(0; 0)$. For a sufficiently high nonreceptor-to-receptor ratio, $Z \approx 1$, binding of morphogens with nonreceptors dominates, resulting in the graphs for normalized signaling *Dpp* gradients in Figure 3, showing the effects of high receptor occupancy but low nonreceptor occupancy. The presence of nonreceptors not only reduces the magnitude of enhanced signaling morphogen gradient (bringing it closer to the one for the normal morphogen synthesis rate) but also makes the gradient more convex.

The change from a decreasing but nearly linear signaling gradient in the interval $(0, 1)$ to a convex one reflects the dominant effect due to a relatively high concentration of nonreceptors toward a state of low nonreceptor occupancy (as shown mathematically in the previous section). The reduced

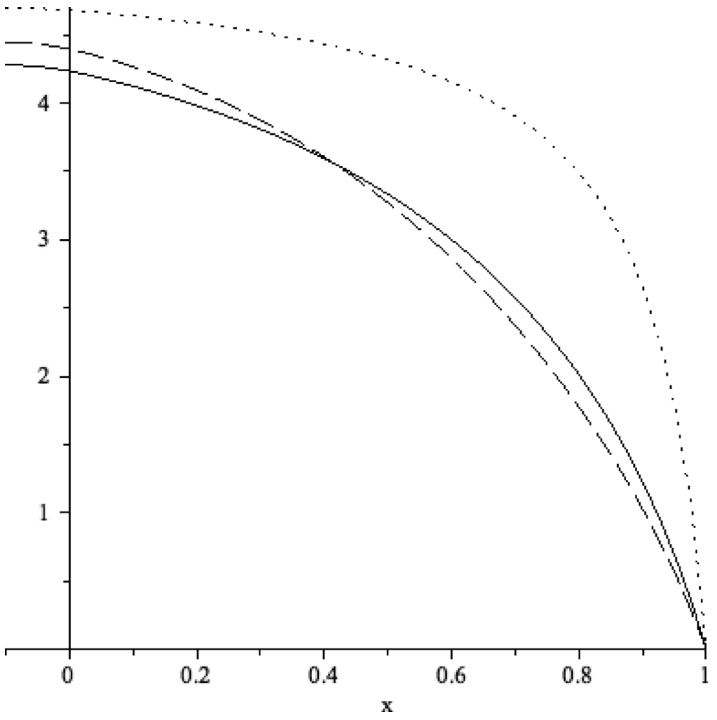

Figure 4. Signaling gradients for system reported in Table 2 for $Z = 0.5$. (solid $= \bar{b}(x, 0)$, dashed $= \tilde{b}(x, 1)$, dots $= \tilde{b}(x, 0)$).

concentration magnitude and higher degree of convexity should render the enhanced gradient more in line with the normal one, the enhanced synthesis rate notwithstanding. To the extent that more nonreceptors further reduce the magnitude of the signaling gradient concentration and make it even more convex, it is not surprising that the *robustness index* R_b as a function of Z first decreases with Z to reach a minimum and then reverses itself and increases with more nonreceptors. From Table 1, we see that for the prescribed level of morphogen synthesis rate, the system is most robust around $Z = 1$.

Table 2 shows the corresponding results for the same morphogen system reported in Table 1 except for a larger prescribed $\bar{V}_L$. The computed values for $\tilde{r}_0(Z) = \tilde{r}(0; Z)$ and $\tilde{n}_0(Z) = \tilde{n}(0; Z)$ show that neither receptors nor nonreceptors are in a state of low occupancy. These are also reflected in the graphs for $\bar{b}(x; 0)$, $\tilde{b}(x; 0)$ and $\tilde{b}(x; Z)$ in Figure 4. Nevertheless, a modest level of nonreceptors brings the enhanced gradient $\tilde{b}(x; Z)$ to nearly coincident with $\bar{b}(x; 0)$ with both robustness indices well within the acceptable threshold 0.2. In contrast to that for the previous example, both indices provide nearly the same global indicator for normal development.

7. Concluding remarks

In this paper, we initiated a quantitative investigation of the effects of cell surface bound nonreceptors and their role in promoting robustness of signaling morphogen gradients by investigating an extracellular model more realistic than the one in [20]. Nonreceptor-mediated degradation as a possible mechanism for promoting robustness relative to significant morphogen synthesis rate change is suggested by the numerical simulations in [12]. The principal goal of the present paper is to validate theoretically the inference from the numerical experiments. To this end, the basic model of morphogen gradient formation in wing imaginal disc formulated and analyzed in [17] is extended to include reversible binding with nonreceptors (synthesized at a prescribed rate) and nonreceptor mediated degradation of nonreceptor-bound morphogens. It is shown that the signaling morphogen gradient of this model is, as expected, enhanced by an increase in morphogen synthesis rate (to result in abnormal development). This enhancement is shown to diminish as the nonreceptor synthesis rate increases while the receptor synthesis rate is kept fixed.

Beyond the validation of nonreceptor-mediated degradation as a possible mechanism for robustness of signaling morphogen gradient with respect to a significant increase in morphogen synthesis rate, the results obtained also quantify the level of nonreceptor synthesis rate needed to achieve a level of insensitivity to morphogen dosage. It is possible that a given wing disc with a certain set of system characteristics (associated with the specific values of the rate constants) may require a biologically unrealistic level of nonreceptors for robustness. In that case, robustness cannot be attained even if it is theoretically possible. Hence, it is important to delineate the relation among the system characteristics including the nonreceptor-to-receptor ratio. This task has been undertaken recently; some preliminary results can be found in [9–12].

In this paper, we work with a simple but realistic model to obtain explicit solutions by perturbation and asymptotic methods. They enable us to show how the addition of nonreceptors changes an enhanced signal gradient by

- reducing the magnitude of the gradient,
- making the slope of the gradient more negative, and
- rendering the gradient more convex.

So that the enhanced gradient from an enhanced morphogen synthesis rate may be reduced to a tolerable level (for normal development) for some range of nonreceptor concentrations.

For systems for which perturbation and asymptotic solutions are not appropriate, accurate numerical solutions for the various gradients and robustness measures are obtained. In general, the signaling robustness index

$R_b(Z)$ tends to exaggerate the possibility of abnormal development compared to the displacement index $R_x(Z)$. However, the numerical results show a general qualitative agreement between the two different robustness indice, espccially on the optimal level of nonreceptor concentration for robustness.

Whatever the concentration of nonreceptors during normal development, environmental perturbations that lead to an enhanced signaling gradient require additional nonreceptors to degrade the excess moorphogen to maintain normal development. An appropriate feedback mechanism for stimulating such an enhanced degradation will be a subject of a future publication.

Acknowledgment

The research is supported in part by NIH Grants R01GM067247, and P50-GM076516. The NIH R01 grant was awarded through the Joint NSF/NIGMS Initiative to support research in the area of mathematical biology. The author is also a member of the NIH supported UCI Center for Complex Biological System (CCBS) and the Center for Mathematical and Computational Biology (CMCB).

References

1. G. von Dassow, E. Meir, E. M. Munro, and G. M. Odell, The segment polarity network is a robust developmental module. *Nature* 406:188–192 (2000).
2. A. Eldar, R. Dorfman, D. Weiss, H. Ashe, B. Z. Shilo, and N. Barkai, Robustness of the BMP morphogen gradient in Drosophila embryonic patterning. *Nature* 419:304–308 (2002).
3. G. von Dassow and G. M. Odell, Design and constraints of the Drosophila segment polarity module: Robust spatial patterning emerges from intertwined cell state switches. *J. Exp. Zool.* 294:179–215 (2002).
4. B. Houchmandzadeh, E. Wieschaus, and S. Leibler, Establishment of developmental precision and proportions in the early Drosophila embryo. *Nature* 415:798–802 (2002).
5. A. Eldar, D. Rosin, B. Z. Shilo, and N. Barkai, Self-enhanced ligand degradation underlies robustness of morphogen gradients. *Dev. Cell.* 5:635–646 (2003).
6. A. Eldar, B. Z. Shilo, and N. Barkai, Elucidating mechanisms underlying robustness of morphogen gradients, *Curr. Opin. Genet. Dev.* 14:435–439 (2004).
7. N. T. Ingolia, Topology and robustness in the Drosophila segment polarity network, *PLoS Biol.* 2:e123 (2004).
8. O. Shimmi, D. Umulis, H. Othmer, and M. O'Connor, Facilitated transport of a Dpp/Scw heterodimer by Sog/Tsg patterns the dorsal surface of the Drosophila blastoderm embryo, *Cell* 120(6): 873–886 (2005).
9. A. D. Lander, Q. Nie, B. Vargas, and F. Y. M. Wan, Size-normalized robustness of Dpp gradient in Drosophila wing imaginal disc, *JoMMS* 6:321–350 (2011).
10. J.-Z Lei, F. Y. M. Wan, A. D. Lander, and Q. Nie, Robustness of signaling gradient in Drosophila wing imaginal disc, *J. Discret. Contin. Dyn. Syst., Series B* 16(3): 835–866 (2011).

11. J.-Z LEI, D. WANG, Y. SONG, Q. NIE, and F. Y. M. WAN, Robustness of morphogen gradients with "Bucket Brigade" transport through membrane-associated non-receptors, *J. Discret. Contin. Dyn. Syst., Series B* 18(3): 721–739 (2013).
12. A. D. LANDER, F. Y. M. WAN, and Q. NIE, *Multiple paths to morphogen gradient robustness*, CCBS preprint, University of California, Irvine (2005).
13. E. V. ENTCHEV, A. SCHWABEDISSEN, and M. GONZALEZ-GAITAN, Gradient formation of the TGSF-beta homolog Dpp, *Cell* 103:981–991(2000).
14. J. B. GURDON and P. Y. BOURILLOT, Morphogen gradient interpretation, *Nature* 413:797–803 (2001).
15. A. D. LANDER, Q. NIE, and F. Y. M. WAN, Do morphogen gradients arise by diffusion? *Dev. Cell* 2:785–796 (2002).
16. A. D. LANDER, Q. NIE, and F. Y. M. WAN, Internalization and end flux in morphogen gradient formation, *J. Comp. Appl. Math*. 190:232–251 (2006).
17. A. D. LANDER, Q. NIE, and F. Y. M. WAN, Spatially distributed morphogen production and morphogen gradient formation, *Math. Biosci. Eng.* 2:239–262 (2005).
18. B. VARGAS, *Leaky boundary, and morphogen gradient formation*, Ph. D. Dissertation, Department of Mathematics, University of California, Irvine, 2007.
19. A. A. TELEMAN and A. M. COHEN, Dpp gradient formation in the Drosophila wing imaginal disc, *Cell* 103:971–980 (2000).
20. A. D. LANDER, Q. NIE, and F. Y. M. WAN, Membrane associated non-receptors and morphogen gradients, *Bull. Math. Bio.* 69:33–54 (2007).
21. K. M. CADIGAN, M. P. FISH, E. J. RULIFSON, and R. NUSSE, Wingless repression of Drosophila frizzled 2 expression shapes the Wingless morphogen gradient in the wing, *Cell* 93:767–777 (1998).
22. T. LECUIT and S. M. COHEN, Dpp receptor levels contribute to shaping the Dpp morphogen gradient in the Drosophila wing imaginal disc, *Development* 125:4901–4907 (1998).
23. M. KHONG and F. Y. M. WAN, Negative feedback in morphogen gradients, *Frontier of Applied Mathematics* (D.-Y. HSIEH, M. ZHANG, and W. SUN, Eds.), pp. 29–51, World Scientific, NJ, 2007.
24. A. D. LANDER, Q. NIE, F. Y. M. WAN, and Y.-T. ZHANG, Localized ectopic expression of Dpp receptors in a Drosophila embryo, *Stud. Appl. Math.* 123:175–214 (2009).
25. Y. LOU, Q. NIE, and F. Y. M. WAN, Effects of Sog on *Dpp*-receptor binding, *SIAM J. Appl. Math.* 65:1748–1771 (2005).
26. C. M. MIZUTANI, Q. NIE, F. Y. M. WAN, Y.-T. ZHANG, P. VILMOS, E. BIER, J. L. MARSH, and A. D. LANDER, Origin of the BMP activity gradient in the Drosophila embryo, *Dev. Cell* 8:1–10 [plus supplement] (2005).
27. D. H. SATTINGER, Monotone methods in nonlinear elliptic and parabolic boundary value problems, *Indiana Univ. Math. J.* 21:981–1000 (1972).
28. H. AMANN, On the existence of positive solutions of nonlinear boundary value problems, *Indiana Univ. Math. J.* 21:125–146 (1971).
29. J. SMOLLER, *Shock Waves and Reaction-Diffusion Equations*, Springer Verlag, New York, 2000.

UNIVERSITY OF CALIFORNIA, IRVINE

(Received July 18, 2013)